

# INVESTIGATING A NEW STRUCTURE FOR OFFSHORE WIND FARM IN DC TRANSMISSION

Alireza Alizadeh Kiapi

Department of Electrical Engineering, K. N. Toosi University of Technology, KNTU, Tehran, Iran

**Abstract:** In this study, a new structure for power transfer in offshore wind farms is proposed. The proposal includes a conventional synchronous generator with excitation coils, a full bridge diode rectifier, which eventually is connected to a HVDC transmission system. The excitation coil is fed by a DC buck converter. Dynamic response of proposed structure is evaluated based on simulation results. Simulation results show that the proposed model can perfectly respond to the wind speed variation.

**Keywords:** Synchronous generator, Full bridge rectifier, buck converter, HVDC, wind speed, MPPT

## I. INTRODUCTION

The environmental pollution caused by the increasing use of fossil fuels to provide energy and heating, made the movement towards the use of renewable energies. At the meantime, wind energy has attracted much attention from previous decades as one of the cheapest as well as oldest green energy used to produce electrical energy, but at the same time one of the largest renewable energy sources [1].

One part of the wind turbines that has changed over the years is the electrical one. These changes have led to the creation of a variety of wind turbines with characteristics such as constant speed or variable speed, small or large rated power, specially designed for connecting to a power grid or work in the island state, and finally for wind farms, land or sea [2].

The initial wind turbines used a Fixed Speed Induction Generator (FSIG), which were used at a constant speed of less than 3% slip. This structure encountered problems like mechanical rotor speed fluctuations, which made them harder to control. Therefore, variable speed turbines were provided with the rotor's external resistance, but these turbines also had a high loss in the resistors and the limited range of speed control. With the increasing need for variable speed operation of wind turbines, different electrical machines are being studied for wind turbine application. In [3] DFIG is proposed as a variable speed electrical machine in which the mechanical losses corresponding to the gearbox is eliminated. Using of double fed induction generators (DFIGs) is more common in large turbines. As the nominal power of the converter used in this type of turbine is a fraction of DFIG nominal power, the advantage lower cost in using DFIG for variable speed structure is obtained [4]. However, the problem with the DFIG structure is more in the use of slip ring. In Fig. 1 wind turbines used in an offshore wind farm are shown. With the disclosure of the economical benefits of such offshore wind farms, the attitude toward these fields changed. Those benefits include:

- According to the research, the average wind speed at sea is significantly higher than the average wind speed in the land [5].

- Due to the lack of physical barriers at sea, changes in wind speed at sea are less than land, which means more uniform production on sea farms than land farm. This result in less uncertainty and therefore less requirement for reserve at system level in wind generation [6][7].

- It is easy to find the right place to build a wind farm at sea while the proper locations for the wind farm are limited.

- Unlike land, wind speed becomes more intense in the afternoon in the sea, which is more consistent with more electric energy consumption in the afternoon in both residential and commercial demand. At these times, conventional power plants are near the maximum and the load is at its least flexibility due to comfort issues [8][9].

- There are offshore wind farms near the major energy consumer centers (for example, in the South East of England and New York in the United States), while the implementation of land-based wind farms in these areas faces many problems due to limitations.

- With the disappearance of noise limits in marine environments, higher speeds are possible for offshore wind farms, which reduces torque and thus reduces the cost of the mechanical part of the turbine [5][10].



Fig. offshore wind turbine

On the other hand, advancement of electrical storage and demand response technology overcome wind energy uncertainty and boost wind energy integration into the grid[11][12][13]. In this way, it is seen that offshore wind farms are becoming one of the most important types of wind farms and even one of the most important sources of renewable electrical energies, and therefore extensive efforts are being made to increase reliability and reduce their cost.

Moreover, wind turbines can be optimally placed in the buses of the network such that total costs of the system become minimized. In [14], wind turbines are placed and their generation profiles according to the estimation of wind speed are introduced to the system to make the energy losses and total costs of the system as minimum as possible.

Furthermore, during placement planning of wind turbines, their interaction with each other and with conventional generators should be considered power swing reduction [15] and preventing frequency instability in the power system [16].

In this study, a new method for power transfer in offshore wind farms is proposed. Dynamic and transient response of proposed structure is evaluated based on simulation results. This paper is organized as follows; In the next section, a brief overview of the various structures that are currently commonly used for wind farms is presented. In section III the proposed structure for offshore wind farms is introduced. Simulation results are demonstrated in section IV. Finally, the conclusion is given in section V.

## II. OVERVIEW OF WIND FARMS

Different approaches were proposed to adapt the voltage levels of the transmission line and wind turbines. Depending on the proposed solution, the structure of the local network of wind farms can be divided into the following groups:

### A. Local Network with Parallel Turbines

In this structure, the local wind farm network is located at a specific voltage level, and all turbines are at that voltage level and connected to the local network in parallel as a current source. The local network connection to the HVDC transmission line may be carried out either directly or through a DC / DC converter. Normally, such configuration is known as DC microgrid, when different sources are parallel to each other and connected to the DC bus via DC/DC or AC/DC converters [17]

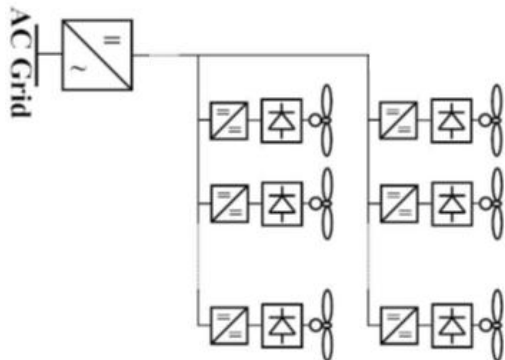


Fig. 1 Use of DC / DC converters at the wind turbine terminal

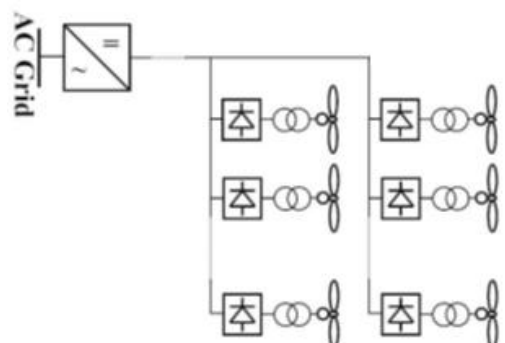


Fig. 2 The use of AC transformers in the AC section of the wind turbine structure

### A.1 Parallel Turbines with Increasing Voltage Level in Turbines Themselves

In this structure, the voltage level of the local wind farm network is selected at the same level as the transmission line voltage and, in fact, there is a direct electrical connection between the local network and the HVDC transmission line. In this case, wind turbines must be connected directly to a voltage level of several hundred kilovolts; so it needs to increase the voltage level in the turbines terminal. Three solutions can be proposed for this purpose.

### A.2 Use of DC / DC Converters at the Wind Turbine Terminal

In this method, a DC / DC converter at the junction of the wind turbine to the local network is matching the voltage levels of the two sides [18]. In fact, a DC/ DC connector is connected to the generator terminal, where the electrical energy is about a few kV, and increases this DC voltage to a few hundred kilovolts (Fig. 2). The problem with this approach is the high cost and low efficiency of DC/DC converter [19].

### A.3 The Use of AC Transformers in the AC Section of the Wind Turbine Structure

The second solution is according to Fig. 3, in which the increase of the voltage level is carried out inside the wind turbine and by means of a transformer at the generator terminal. What can make it difficult to use this method is that synchronous generators with a large number of poles and with a direct (without gearbox) connection to the wind turbine usually have a normal frequency of less than 50 or 60 Hz in power networks during normal operation. This requires the need for larger-core transformers with more weight.

### A.4 Parallel Turbines by Increasing the Voltage Level at the Junction of Local Network with the HVDC Transmission Line

Another method of matching the voltage levels of the transmission line and the turbines is that the local network voltage level is selected at the level of the rectified output voltage of the wind turbines, and all of the wind turbines of the farm are connected to the local DC network via an inductor (as a current source). Finally, after the electrical energy generated at the farm was collected by the local network, a DC / DC converter is placed at the local network connection point to the transmission line to perform the task of matching the voltage levels of the two sides according to Fig. 4 [20][21]. DC/DC converters can be step up as boost converters [22] or step down as buck converters [23]. In this paper Buck converters will be used.

The problem with this method is the lack of DC / DC converters with a capacity of several hundred megawatts. In this case, the nominal capacity of the DC / DC converter, instead of the capacity of each turbine, should be equal to the total wind farm's capacity.

### B. Local Network with Series Turbines

Another solution that can be used to adapt the voltage levels of the HVDC transmission line and the electric terminal of

the wind turbines is that the increase of the voltage level in the structure of the wind turbines itself does not take place, and each wind turbine at the same level as the turbine generator voltage is connected to the local network. However, the arrangement of wind turbines is in series in a local network rather than parallel, so that the voltage of the wind turbine terminal will be added. In this case, there will be a direct relationship between the nominal voltage of the HVDC transmission line and the nominal voltage of turbine terminals and the number of turbines in a series loop (Fig. 5). The main problem with the application of this method is the control of wind turbines, which should be carried out in such a way that, it can control the voltage of the turbine terminal, so that under the same loop flow for all turbines, the maximum power absorbed by the wind turbine. Besides, the controller of the DC / AC converter on the other side of the HVDC transmission line, which is located on the power grid, should also be able to coordinate with the local turbine controllers to determine the flow of the corresponding loop and simultaneously act on the AC side as well. The most common DC/AC converter used to connect HVDC transmission line to the AC grid is voltage source converter. This converter has PI current controllers and its state equations are discussed in [24].

III. PROPOSED STRUCTURE OFFSHORE WIND FARM

As it is seen in Fig. 6, in the proposed wind farm structure, rectifier converters GTO switches on the wind turbine output are replaced with a full diode bridge rectifier, which is expected to result in a significant reduction in costs. The full bridge diode rectifier connects the new structure via an inductor as a current source to the DC network. On the other hand, the excitation of the rotor of generators is carried out through a DC / DC converter with a nominal power of a percentage of the nominal power of the turbine. It is obvious that the cost of this converter will be negligible with regard to its low nominal power compared to the reduction in the cost of the turbine converter.

A. Dynamic Model of Buck Converter

The state equations can be written as follows while the switch is on:

$$\frac{1}{\omega_b} \frac{d}{dt} \begin{bmatrix} i_L \\ V_c \end{bmatrix} = \begin{bmatrix} 0 & -\frac{1}{L} \\ \frac{1}{C} & 0 \end{bmatrix} \begin{bmatrix} i_L \\ V_c \end{bmatrix} + \begin{bmatrix} \frac{1}{L} & 0 \\ 0 & -\frac{1}{C} \end{bmatrix} \begin{bmatrix} V \\ i_o \end{bmatrix} \quad (1)$$

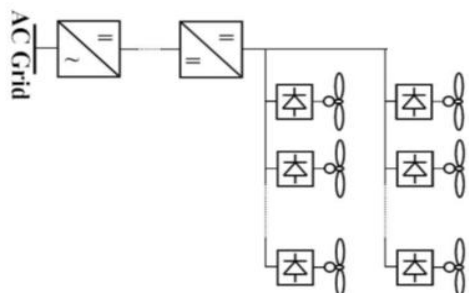


Fig. 3 Increasing the voltage level at the junction of local network with the HVDC transmission line

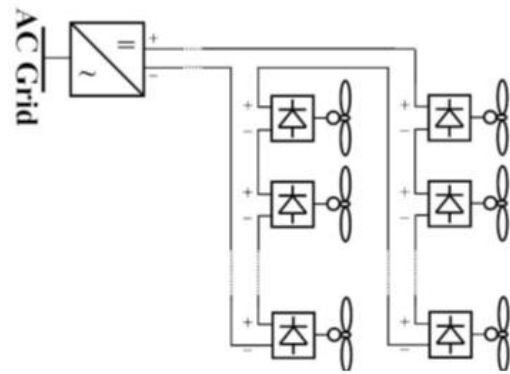


Fig. 4 Local network with series turbines

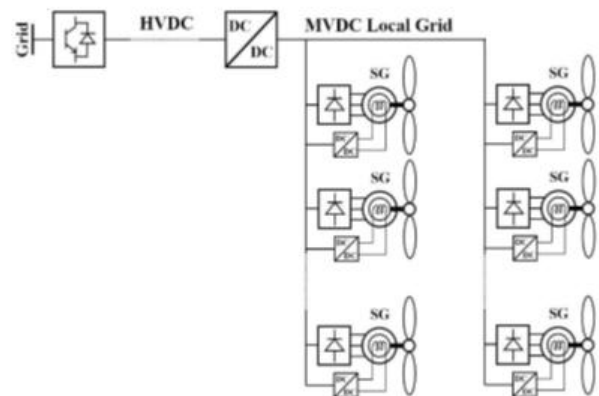


Fig. 5 Proposed structure of offshore wind farm  
 Similarly, when the switch is off, the state equations are as follows:

$$\frac{1}{\omega_b} \frac{d}{dt} \begin{bmatrix} i_L \\ V_c \end{bmatrix} = \begin{bmatrix} 0 & -\frac{1}{L} \\ \frac{1}{C} & 0 \end{bmatrix} \begin{bmatrix} i_L \\ V_c \end{bmatrix} + \begin{bmatrix} 0 & 0 \\ 0 & -\frac{1}{C} \end{bmatrix} \begin{bmatrix} V_g \\ i_o \end{bmatrix} \quad (2)$$

Since the switch is on for  $DT_s$  and it is off for  $(1 - D)T_s$ , regarding the average current, it can be written:

$$\frac{1}{\omega_b} \frac{d}{dt} \begin{bmatrix} \langle i_L \rangle \\ \langle V_c \rangle \end{bmatrix} = \begin{bmatrix} 0 & -\frac{1}{L} \\ \frac{1}{C} & 0 \end{bmatrix} \begin{bmatrix} \langle i_L \rangle \\ \langle V_c \rangle \end{bmatrix} + \begin{bmatrix} \langle D \rangle \frac{1}{L} & 0 \\ 0 & -\frac{1}{C} \end{bmatrix} \begin{bmatrix} \langle V_g \rangle \\ \langle i_o \rangle \end{bmatrix} \quad (3)$$

Where

$$\langle i_L \rangle = \frac{1}{T_s} \int_0^{T_s} i_L(t) dt = I_L + \hat{i}_L \quad (4)$$

Where  $I_L$  is the DC component, and  $\hat{i}_L$  is the oscillation around the operating point. By linearizing the relationship around the operating point and ignoring the second-order terms, it is simplified as:

$$\frac{1}{\omega_b} \frac{d}{dt} \begin{bmatrix} I_L \\ V_c \end{bmatrix} = \begin{bmatrix} 0 & -\frac{1}{L} \\ \frac{1}{C} & 0 \end{bmatrix} \begin{bmatrix} I_L \\ V_c \end{bmatrix} + \begin{bmatrix} D \frac{1}{L} & 0 \\ 0 & -\frac{1}{C} \end{bmatrix} \begin{bmatrix} V_g \\ i_o \end{bmatrix} = 0 \quad (5)$$

$$\frac{1}{\omega_b} \frac{d}{dt} \begin{bmatrix} \hat{i}_L \\ \hat{V}_c \end{bmatrix} = \begin{bmatrix} 0 & -\frac{1}{L} \\ \frac{1}{C} & 0 \end{bmatrix} \begin{bmatrix} \hat{i}_L \\ \hat{V}_c \end{bmatrix} + \begin{bmatrix} D & 0 & \frac{V_g}{L} \\ 0 & -\frac{1}{C} & 0 \end{bmatrix} \begin{bmatrix} \hat{V}_g \\ \hat{i}_o \\ \hat{D} \end{bmatrix} \quad (6)$$

If we consider the input current of the converter as the output of this state space:

$$\langle i_m \rangle = \langle D \rangle \langle i_L \rangle \quad (7)$$

It can be written with linearizing as:

$$\hat{i}_m = D \hat{i}_L + \hat{D} i_L \quad (8)$$

Given that the output voltage of the converter is actually the generator excitation, the capacitor voltage is written according to the inputs as:

$$\hat{V}_c = \frac{\frac{D \omega_b^2 \hat{V}_g + \left(-\frac{s}{c}\right) \hat{i}_o + \frac{V_g \omega_b^2 \hat{D}}{LC}}{s^2 + \frac{\omega_b^2}{LC}} \quad (9)$$

Assuming that the input voltage changes are zero and small, the only changes are related to the coefficient of duty cycle. Now, changes in the coefficient of duty cycle are to be calculated. In general, the duty cycle is calculated from the comparison of a control signal with a saw tooth signal. Such a structure is shown in Fig. 7.

In this situation, the coefficient of duty is equal to:

$$d(t) = \frac{v_{co}(t)}{v_m}, 0 < v_{co} < v_m \quad (10)$$

It can be written dynamically as:

$$D + \hat{D} = \frac{V_{co}}{V_m} + \frac{\hat{V}_{co}}{V_m} \quad (11)$$

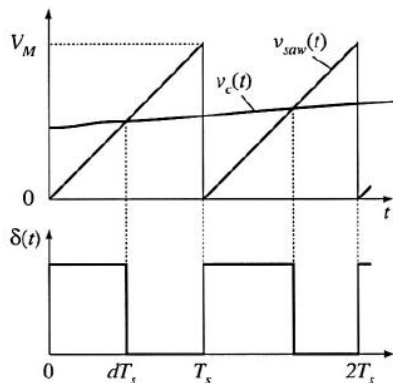


Fig. 6 Duty cycle of buck converter

By inserting the corresponding relationships, the general function can be written as:

$$\hat{e}_{fd} = -\frac{\omega_b}{c} \cdot \frac{s}{s^2 + \omega_{buck}^2} \hat{i}_{fd} + \frac{\omega_{buck}^2}{s^2 + \omega_{buck}^2} \cdot \frac{V_g}{V_m} \hat{V}_{co} \quad (12)$$

Where  $\omega_{buck} = \frac{\omega_b}{\sqrt{LC}}$  is the natural frequency of the converter. If the values L and C are given, this frequency is equal to:

$$\omega_{buck} = 0.4 f_s \quad (13)$$

Which will be 4 KHz. With larger L and C in the converter, this frequency will decrease. It may seem that such a system is not attenuated. Assume the excitation current is as follows:

$$\hat{e}_{fd} = R_{fd} \hat{i}_{fd} + \hat{e}_{load} \Rightarrow \hat{i}_{fd} = \frac{\hat{e}_{fd}}{R_{fd}} + \hat{i}_{load} \quad (14)$$

By inserting the excitation current in relation (12), it can be written:

$$\hat{e}_{fd} = -\frac{\omega_b}{c} \cdot \frac{s}{s^2 + 2\xi\omega_{buck} + \omega_{buck}^2} \hat{i}_{load} + \frac{\omega_{buck}^2}{s^2 + 2\xi\omega_{buck} + \omega_{buck}^2} \cdot \frac{V_g}{V_m} \hat{V}_{co} \quad (15)$$

Where  $\xi$  is the damping factor and defined as:

$$\xi = \frac{\omega_b}{2R_{fd}c\omega_{buck}} = \frac{1}{2R_{fd}} \sqrt{\frac{L}{C}} \quad (16)$$

Given the low range of variations, it is possible to expect the response to be without fluctuation. In general, the excitation voltage is written as follows:

$$\hat{e}_{fd} = -Z_{out} \hat{i}_{load} + G_{vd} \cdot \frac{1}{V_m} \hat{V}_{co} \quad (17)$$

### B. Removing the Dynamic of Buck Converter

Fortunately, the buck converter's poles are so large that its time delay in the mechanical equations and the internal oscillations of the generator is completely overlooked. The Buck converter model is shown in Fig. 8.

Where  $G_c$  is the controller and H is the sensor transfer function. In general, if T (s) is the open loop transfer function and is equal to:

$$T(s) = H(s)G_c(s)G_{vd}(s) \frac{1}{V_m} \quad (18)$$

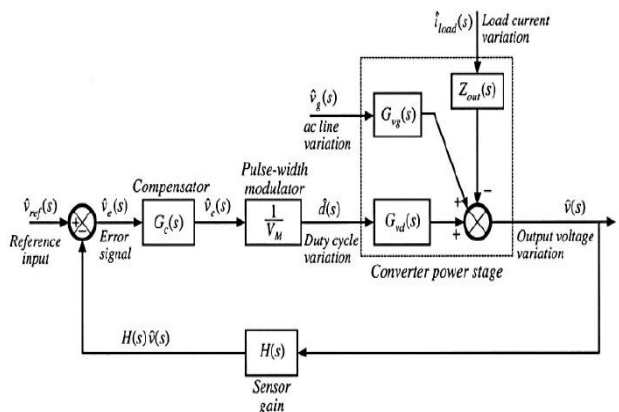


Fig. 7 Buck converter model

Then it can be written:

$$\hat{V} = \hat{V}_{ref} \frac{1}{H} \frac{T}{1+T} + \hat{V}_g \frac{G_{vg}}{1+T} - \hat{i}_{load} \frac{Z_{out}}{1+T} \quad (19)$$

It can be written that:

$$\frac{T}{1+T} \approx \begin{cases} 1 & \text{for } |T| \ll 1 \\ T & \text{for } |T| \gg 1 \end{cases} \quad (20)$$

$$\frac{1}{1+T(s)} \approx \begin{cases} \frac{1}{T(s)} & \text{for } |T| \ll 1 \\ 1 & \text{for } |T| \gg 1 \end{cases} \quad (21)$$

T is always such that at small frequencies it is large and small at large frequencies. Therefore, at low and zero

frequencies, the output voltage is completely matched the reference voltage and also is less effected by output current and the input voltage variations. At the same time, at high frequencies, the output voltage is completely dependent on the fluctuations of the output current and the input voltage and can not be controlled by the reference voltage.

C. Wind Power Modelling

Wind energy is converted to mechanical energy by rotating the turbine rotor. The mechanical power delivered by the wind to the turbine is a function of wind speed, angle of the blades and the speed of the turbine. In the permanent state, the mechanical power delivered by the wind is expressed by the following relation [25]:

$$P_{mec} = \frac{\rho}{2} A_r V_w^3 C_p(\lambda, \beta) \tag{22}$$

$P_{mec}$  is the absorbed mechanical power,  $\rho$  is the air density in  $Kg / m^3$ ,  $A_r$  is the area swept by the rotor blades,  $V_w$  is the wind speed in m/s and  $C_p$  is the aerodynamic efficiency, which is a function of  $\lambda$ , the tip speed ratio, and  $\beta$ , the angle of the blades.  $\lambda$  is defined as:

$$\lambda = \frac{D_r}{2} \cdot \frac{\omega_{wt}}{V_w} \tag{23}$$

Where  $D_r$  is the diameter of the rotor and  $\omega_{wt}$  is the turbine rotor speed in rad/s. Relations (22) and (23) can be simpler as follows:

$$P_{mec} = K_2 V_w^3 C_p(\lambda, \beta) \tag{24}$$

$$\lambda = K_1 \frac{\omega_{wt}}{V_w} \tag{25}$$

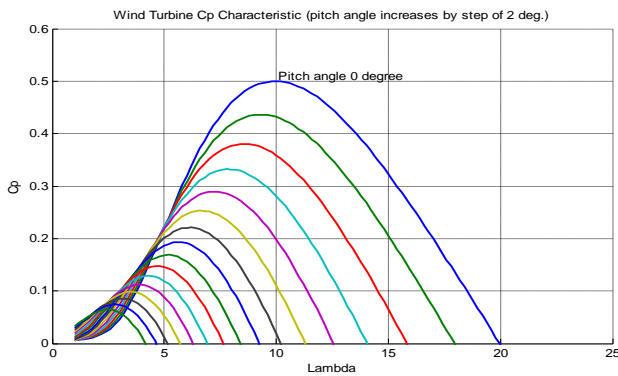


Fig. 8 Aerodynamic efficiency curve

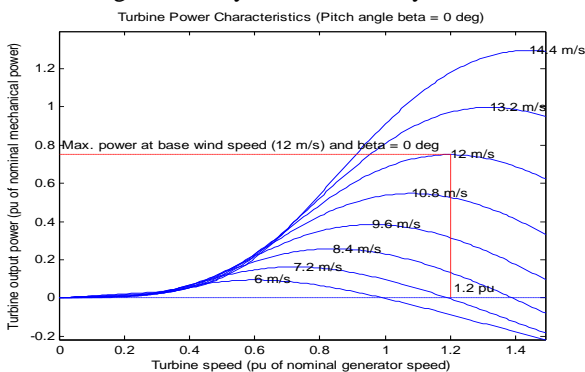


Fig. 9 wind power in different wind and turbine speed

The aerodynamic efficiency is a function of the tip speed ratio and pitch angle, which is plotted in Fig. 9 in terms of  $\lambda$  and zero-degree pitch angle. Increasing the pitch angle in high wind speeds reduces the absorbed power.

Finally, after calculating the output power of the turbine by the relations (24) and (25), the shaft torque is calculated as:

$$T_{wt} = \frac{P_{mec}}{\omega_{wt}} \tag{26}$$

In Fig. 10 wind power is plotted at various wind speeds as well as various generator speeds. As can be seen, at a certain wind speed, there is a turbine speed at which the power generated by the generator is maximal. The maximum turbine speed is limited to 1.2

D. Turbine Controller Model

In this section, the maximum turbine power tracker module will be described. The function of this module is to adjust the angle of the blades, as well as to determine the reference power to track the maximum power [26][27]. The maximum power tracker curve is shown in Fig. 11. This curve is limited between the speeds of 0.7 pu to 1.2 pu. This module has a duty to measure the speed at any moment and calculates the maximum power based on the turbine speed, and by estimating the losses and reducing it from the calculated value, generates the reference power and delivers it to the controller.

Typically, the amount of reference power variation is limited by a limiting change rate to prevent high output power fluctuations. That means:

$$\frac{dp_{ref}}{dt} = k \tag{27}$$

The value of K has a significant effect on the output power ripple. The smaller the K value, the lower the ripple power, and in turn, the maximum power tracing speed is reduced, and the larger the K, the faster the tracking speed and the more is the power ripple. Here, the K value is set to 0.01 for the maximum reduction of the ripple. This means that it takes 10 seconds to change the reference power to only 0.1.

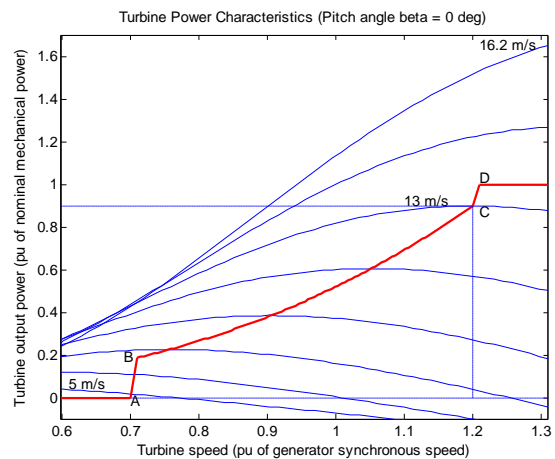


Fig. 10 MPPT curve

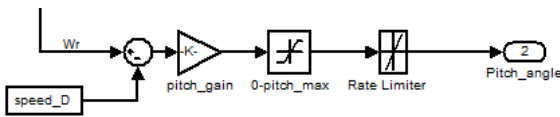


Fig. 11 Pitch angle control

The other function of this module is to adjust the angle of the blades, which at high speeds increasing the angle of the blade, reducing the power consumption and reducing the speed. The pitch angle controller is shown in Fig. 12.

The difference between the actual velocity and velocity at point D is determined by a coefficient. The angle of the blade is between 0 and 45 degrees and its rate of change is 2 degrees per second.

E. Modeling the Mechanical Actuator

The mechanical equations are presented as follows:

$$\omega_{wt} = \frac{1}{2H_{wt}} \int (T_{wt} - T_m) dt \quad (28)$$

$$T_m = K_{sh} \cdot \omega_b \int (\omega_{wt} - \omega_r) dt + K_D (\omega_{wt} - \omega_r) \quad (29)$$

$H_{wt}$  is a constant of inertia, and here it is assumed to be 4 seconds.  $K_{sh}$  is a coefficient of stiffness equal to 1.05 and  $K_D$  is a damping coefficient equal to 1.5.

IV. SIMULATION RESULTS

In this section, the system response to wind speed variation and MPPT is studied.

A. System Response to Wind Speed Fluctuations

In this section, the system response to a fluctuation in wind speed is investigated. The waveforms are shown in Fig. 13. The wind speed decreases from 12 to 10 at  $t=40$  (s) and remains at this value till  $t=45$  (s). At this time, the output power is reduced from 0.7 to 0.55. However, in normal conditions, the power should be reduced by 0.4.

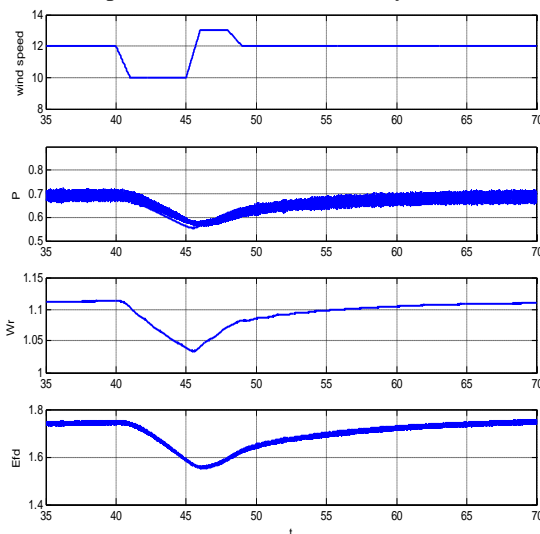


Fig. 12 System responses to wind fluctuations

Simulation results indicate that output power is following the reference power perfectly, and therefore, if there is a power reduction, it results from the reduction of reference power. The turbine speed also decreases from 1.11 to 1.03 and increases with increasing wind speed. Although the output power follows well the reference value, the power output has high ripples.

The excitation voltage also decreases with decreasing reference power and increases with increasing reference power. The simulation results clearly show the stability of the control system. The time to reach a constant value is about 10 seconds, which is actually proportional to the cutoff frequency of the transfer function  $T(s)$ , i.e., 0.1 Hz.

B. System Response to Maximum Power Tracking

In this section, the system responds to a permanent change in wind speed is investigated. The waveforms are shown in Fig. 14. The wind speed rises from 12 m/s to 13 m/s at  $t=40$  (s) and remains at this value. As it is shown in Fig. 14 it takes about 10 seconds to reach its final value.

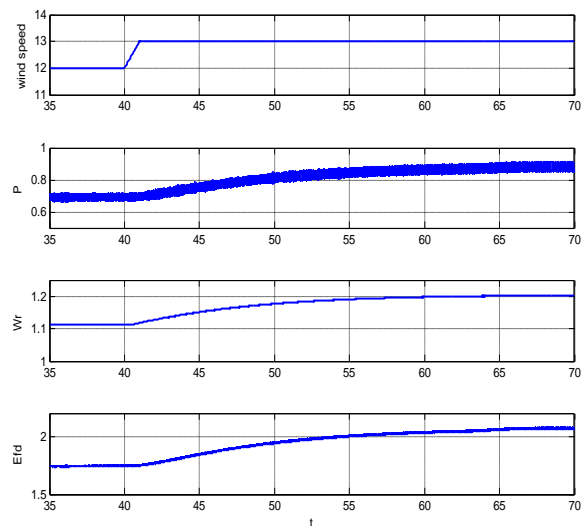


Fig. 13 system response corresponding to MPPT

As the wind speed increases, the torque increases, and resulting in a higher speed, whereas the power is almost constant. As the speed increases, the reference power increases, and the power output increases with reference power and is less affected by the torque produced by the wind.

As can be seen in the first moments of increase in wind speed, the excitation voltage is almost constant so that the output power does not change. But then, as the wind speed increases, the excitation voltage also increases.

V. CONCLUSIONS

In this paper, the proposed model for wind turbine electrical part and the method of matching the transmission of wind turbines and lines are introduced. Then the system is modeled using the state space of the system. The linearized model is simulated to evaluate its accuracy. Dynamic response of proposed structure is evaluated based on

simulation results. Simulation results show that the proposed model can perfectly respond to the wind speed variation.

#### REFERENCES

- [1] Fujin Deng and Zhe Chen "An offshore wind farm with DC grid connection and its performance under power system transients" Power and Energy Society General Meeting, IEEE, 2011.
- [2] Hau, E. "Wind Turbines Fundamentals, Technologies, Application, Economics" 2nd Edition, Springer, 2005.
- [3] M. Ghanaatian, A. Radan, "Modeling and simulation of Dual Mechanical Port machine" International Power Electronics, Drive Systems and Technologies Conference (PEDSTC), pp. 125-129, 2013.
- [4] Polinder, H., et al. "Comparison of direct-drive and geared generator concepts for wind turbines", IEEE Transactions on Energy Conversion, Vol. 21, no. 3, pp. 725-733, 2006.
- [5] Wu, Guohong, Y. Tohbai, and T. Takahashi. "Construction and operational properties of offshore wind farm power generation system with self-commutated HVDC transmission." In Power System Technology (POWERCON), 2010 International Conference on, pp. 1-6. IEEE, 2010.
- [6] M. S. Modarresi and L. Xie, "An operating reserve risk map for quantifiable reliability performances in renewable power systems," 2014 IEEE PES General Meeting Conference & Exposition, National Harbor, MD, 2014, pp. 1-5.
- [7] J. B. Cardell and C. L. Anderson, "A flexible dispatch margin for wind integration," IEEE Transactions on Power Systems, vol. 30, no. 3, pp. 1501–1510, 2015.
- [8] W. Jewell, "Residential energy efficiency and electric demand response," in 2016 49th Hawaii International Conference on System Sciences (HICSS), Jan 2016, pp. 2435–2444.
- [9] M. S. Modarresi, L. Xie, and C. Singh "Reserves from Controllable Swimming Pool Pumps: Reliability Assessment and Operational Planning," in 51st Hawaii International Conference on System Sciences (HICSS), January 2018.
- [10] Das, D., J. Pan, and S. Bala. "HVDC Light for large offshore wind farm integration." In Power Electronics and Machines in Wind Applications (PEMWA), 2012 IEEE, pp. 1-7. IEEE, 2012.
- [11] Amini, Mahraz, and Mads Almassalkhi. "Trading off robustness and performance in receding horizon control with uncertain energy resources." Power Systems Computation Conference (PSCC). 2018.
- [12] Wang, Zhongyang, et al. "Research on the active power coordination control system for wind/photovoltaic/energy storage." Energy Internet and Energy System Integration (EI2), 2017 IEEE Conference on. IEEE, 2017.
- [13] S. Jafarishiadeh, M. Farasat "Modeling and Sizing of an Undersea Energy Storage System", IEEE Transactions on Industry Applications, vol. 54, no. 3, pp. 2727-2739, 2018.
- [14] N. Ghanbari, H. Mokhtari, S. Bhattacharya, "Optimizing Operation Indices Considering Different Types of Distributed Generation in Microgrid Applications", Energies 2018, 11, 894.
- [15] H.Gharibpour, H. Monsef, M.Ghanaatian, "The comparison of two control methods of power swing reduction in power system with UPFC compensator", Iranian Conference on Electrical Engineering (ICEE), pp. 386-391, 2012.
- [16] Amini, Mahraz, and Mads Almassalkhi. "Investigating delays in frequency-dependent load control." Innovative Smart Grid Technologies-Asia (ISGT-Asia), 2016 IEEE. IEEE, 2016.
- [17] N. Ghanbari, M. Mobarrez, S. Bhattacharya, "Modeling and Stability Analysis of a DC Microgrid Employing Distributed Control Algorithm", IEEE 8th International Symposium on Power Electronics for Distributed Generation Systems (PEDG), Charlotte, NC, USA, 2018.
- [18] Zhou, Y., et al. "Comparison of DC-DC converter topologies for offshore wind-farm application" 6th IET International Conference on Power Electronics, Machines and Drives, PEMD 2012.
- [19] Jovcic, D. and N. Strachan "Offshore wind farm with centralised power conversion and DC interconnection." Generation, Transmission & Distribution, IET, Vol 3, Issue 6: 586-595, 2009.
- [20] Bahirat, H. J., et al. "Comparison of wind farm topologies for offshore applications" Power and Energy Society General Meeting, IEEE, 2012.
- [21] S. Jafarishiadeh, M. Farasat, S. Mehraeen "Grid-connected operation of direct-drive wave energy converter by using HVDC line and undersea storage system" in Proc.Energy Conversion Congress and Exposition (ECCE), Cincinnati, OH, USA, pp. 5565-5571, 2017.
- [22] P. M. Shabestari, G. B. Gharehpetian, G. H. Riahy and S. Mortazavian, "Voltage controllers for DC-DC boost converters in discontinuous current mode," 2015 International Energy and Sustainability Conference (IESC), Farmingdale, NY, 2015, pp. 1-7.
- [23] Yousefzadeh, E. Alarcon, D. Maksimovic, "Three-level buck converter for envelope tracking applications," IEEE Transactions on Power Electronics, vol. 21, no. 2, pp. 549–552, 2006.
- [24] P. M. Shabestari, S. Ziaeinejad and A. Mehrizi-Sani, "Reachability analysis for a grid-connected voltage-sourced converter (VSC)," 2018 IEEE Applied Power Electronics Conference and Exposition (APEC), San Antonio, TX, 2018, pp. 2349-2354.
- [25] Kawaguchi, T., et al. "Offshore-Wind-Farm Configuration Using Diode Rectifier With MERS in Current Link Topology." IEEE Transactions on Industrial Electronics, Vol 60, Issue 7: 2930-2937, 2013.

- [26] M. a. Abdullah, a. H. M. Yatim, C. W. Tan, and R. Saidur, "A review of maximum power point tracking algorithms for wind energy systems," *Renew. Sustain. Energy Rev.*, vol. 16, no. 5, pp. 3220–3227, Jun. 2012.
- [27] M. A. Abdullah and A. H. M. Yatim, "A study of maximum power point tracking algorithms for wind energy system," in *2011 IEEE Conference on Clean Energy and Technology (CET)*, 2011, pp. 321–326.